BMC Oral Health

RESEARCH

Open Access

Effect of various solvents on the repairability of aged CAD/CAM provisional restorative materials with flowable resin composite: an in vitro study

Peeraya Chitpattanakul[1], Wisarut Prawatvatchara[2*], Nareudee Limpuangthip[2], Awutsadaporn Katheng[3], Pithiwat Uasuwan[4] and Kwanwong Boonpitak[5]

Abstract

Background Increased bond strength between aged CAD/CAM (Computer-Aided Design and Computer-Aided Manufacturing) provisional restorative materials is essential for reparability. This study investigated the impact of three different solvents and airborne-particle abrasion on the shear bond strength (SBS) of aged CAD/CAM provisional restorative materials, which are milled PMMA and 3D-printed resin with flowable resin composite.

Methods 3D-printed resin and milled PMMA ($N=160$ per type) were fabricated into cylindrical shapes (5 mm in diameter, 5 mm in height), aged by 5,000 thermocycling cycles, and randomize divided at random into five groups ($N=32$) based on surface modification protocols: control; non-surface modification, MEK; application with methyl ethyl ketone, THF; application with tetrahydrofuran, Alc; application with isopropyl alcohol, and APA; airborne-particle abrasion with 50-µm alumina oxide particle. The shear bond strength was tested by a universal testing machine with a notch-edged blade placed parallel to the bonded interphase and a crosshead speed of 1 mm/min until failure occurs. Failure modes analyzed under a ×40 stereomicroscopy. Scanning electron microscopy (SEM) at ×1000 magnification was used to evaluate the qualitative surface morphology ($N=2$). The surface roughness was measured using a noncontact surface roughness analyzer at ×50 magnification ($N=10$). A high-performance adsorption analyzer was used to determine the specific surface area ($N=10$), and the data were analyzed two-way ANOVA with Bonferroni post-hoc test.

Results SBS results (mean (95% confidence interval) in MPa) revealed that for both the 3D-printed resin and milled PMMA, the samples in the MEK (3D-printed, 23.2 (21.1–25.2); milled, 16.9 (15.3–18.5)), THF (3D-printed, 27.2 (26.0–28.5); milled,18.4 (16.8–20.0)), and APA groups (3D-printed, 27.9 (26.1–29.8); milled, 19.0 (17.2–20.7)) had significantly greater SBSs than did the samples in the Alc (3D-printed, 16.1 (14.4–17.7); milled, 12.2 (10.5–13.9)) and control groups (3D-printed, 11.7 (10.3–12.9); milled, 11.6 (10.8–12.4)). Compared with milled PMMA, 3D-printed resin presented a greater SBS across all surface modifications, except in the control group, where milled PMMA performed better. Failure

*Correspondence:
Wisarut Prawatvatchara
Wisarut.p@chula.ac.th

Full list of author information is available at the end of the article

mode analysis revealed total adhesive failure in the control and Alc groups, whereas APA resulted in 50% cohesive failure, mixed failure was shown more in 3D-printed resin THF and MEK groups (30%) compared to milled PMMA, THF and MEK group groups (10%). SEM analysis indicated that surface modifications produced rougher surfaces, The surface roughness (μm) was highest in the APA groups for both materials (3D-printed, 1834.2 (1803.8–1864); milled, 1052.8 (1027.0–1078.5)). The specific surface area (m^2/g) was highest in the THF (5.22 (5.18–5.26)), MEK (5.18 (5.11–5.25)) and APA groups (5.17 (5.07–5.26)) of milled PMMA, but in the 3D-printed resin, the THF (4.95 (4.84–5.07)) and MEK groups (4.83 (4.77–4.89)) exhibited highest specific surface area.

Conclusion The application of APA techniques and surface modification using THF and MEK solvents can enhance the shear bond strength of aged milled PMMA and 3D-printed resin provisional restorative materials to flowable resin composites, as compared to the Alc and control groups. Additionally, the effectiveness of the surface modification of APA, THF, and MEK is indicated by dominant cohesive and mixed failure. SEM, surface roughness, and specific surface area indicated that surface morphology change in both CAD/CAM provisional restorative materials.

Keywords Solvent modification, 3D-printed resin, Milled PMMA, Repairability, Shear bond strength

Introduction

Provisional restorations play a crucial role in restorative procedures, as they allow periodontium preservation, pulp tissue protection, tooth movement restriction, occlusal stabilization, and preservation of an appearance that anticipates the outcome of the final restoration [1].

The use of computer-aided design and computer-aided manufacturing (CAD/CAM) has become widely accepted in restorative dentistry and prosthodontics because of its repeatability and time-saving benefits. In the realm of fixed prosthodontics, CAD/CAM systems show outstanding potential in assisting in achieving the desired prosthesis contour and optimum occlusion for patients. The manufacturing of CAD/CAM provisional restorations can be achieved via two techniques: subtractive and additive techniques [2, 3]. The subtractive technique involves milling a pre-polymerized resin composite or polymer block to fabricate restorations. In contrast, the additive technique uses 3D printing to build restorations layer by layer, offering flexibility and customization [4, 5].

In clinical situations, there is a possibility of fractures, wear, or discrepancies in provisional restorations, especially in long-term provisional prostheses such as oral rehabilitation, during radiotherapy, periodontal therapy and implant support prostheses [6, 7]. In such cases, a decision needs to be made regarding whether to repair the existing provisional restoration or fabricate a new one [8]. Even though the direct repair method using resin composites offers clinicians accurate results and simplicity of use, the reparability of aged CAD/CAM provisional restorations remains unclear. To improve bond strength, studies have been conducted on both mechanical and chemical surface modifications, such as diamond bur grinding, airborne-particle abrasion and acid etching, to improve the bonding process of CAD/CAM resin composites [3, 9–13].

Solvents are generally utilized in adhesives to dissolve monomers and enhance bonding efficacy to demineralized dentin substrates, since they facilitate wetting of the dentin surface and displace water present in the moist demineralized dentin matrix [14].

Several dentin bonding resin adhesives contain different solvents, including water, ethanol, and acetone. However, the solvent used in the bonding agent for denture tooth products is methyl ethyl ketone. Solvents like tetrahydrofuran and dimethyl sulfoxide are currently not utilized in commercial adhesives, despite their demonstrated potential in research [15, 16].

For resin composite, the previous study also investigated the effects of solvents in fiber-reinforced composites, hybrid ceramic surface treatments [17, 18] and contaminated resin composites [19]. With respect to repairing aged resin composites, research on the impact of solvents on the surface modification of CAD/CAM provisional restoration materials is limited.

The aim of this study was to investigate the impact of mechanical and three different solvents (methyl ether ketone, isopropyl alcohol, tetrahydrofuran and airborne-particle abrasion) on the shear bond strength between aged CAD/CAM provisional restorative materials, including milled PMMA and 3D-printed to flowable resin composites. The null hypothesis is that there is no difference in the shear bond strength of aged CAD/CAM provisional restorative materials with various surface modifications to flowable composites.

Materials and methods

The sample size was calculated using G*Power version 3.1.9.4 (Faul, Erdfelder, Buchner, and Lang, Heinrich Heine University, Düsseldorf, Germany). Based on a previous study examining the effect of mechanical and chemical surface treatment on the shear bond strength between 3D-printed temporary restoration and auto-polymerized acrylic resin, which reported an effect size of 0.57 [3], an F test for fixed effects in a one-way analysis of variance (ANOVA) was employed. Including a 10%

margin for errors, a sample size of 10 specimens per group was determined to achieve an 80% power and 5% type I error rate for measuring shear bond strength. The materials used in this in vitro experimental study are presented in Table 1, and the experimental flow diagram is shown in Fig. 1.

Preparation of provisional restorative samples

The 3D-printed resin and milled polymethylmethacrylate (PMMA) ($N = 160$ per type) were fabricated into a cylindrical shape with dimensions of 5 mm in height and 5 mm in diameter. The milling process was conducted with a 5-axis dental milling machine (DWX-52D®, DGShape, Roland Company, Hamamatsu, Japan), and 3D-printed resin groups were printed with a digital light processing 3D printer (NextDent 5100 3D printer; NextDent B.V., Soesterberg, Netherlands). Following the manufacturer's instructions, 3D-printed resin was printed vertically with a 50-µm layer thickness, and the post-curing process involved immersion in 95% isopropanol followed by 5 min of rinsing in an ultrasonic bath (5210, Bransonic, Germany) to eliminate excess resin. After 10 min of drying, the samples were subjected to a post-curing process involving 30 min of exposure in an ultraviolet-light curing unit (NextDent LC-3DP Box; 3D Systems) for complete polymerization. All the samples

Table 1 Materials used in this study

Product name and Batch number		Manufacturer	Composition
Milled PMMA	VIPI BLOCK TRILUX Monocolor A3 (0000198441)	Dental Vipi Ltda., Pirassununga, SP, Brazil	Polymethyl methacrylate, pigments, EDMA, Fluorescent
3D-printed resin	Nextdent C&B MFH A3 (WT162N03)	Nextdent, Soesterberg, The Netherlands	Methacrylic oligomer (> 60% w/w), Glycol methacrylate (15–20% w/w), Phosphine oxide (< 2.5%), inorganic filler, Pigment
Adhesive agent	Scotchbond universal plus adhesive (9020276)	3 M, ESPE, St. Paul, MN, USA	2-Propenoic acid, 2-methyl-, diesters with 4,6-dibromo-1,3-benzenediol 2-(2 hydroxyethoxy)ethyl 3-hydroxypropyl diethers (25–35%), 2-Hydroxyethyl Methacrylate (15–25%), 2-Propenoic acid, 2-methyl-, reaction products with 1,10-decanediol and phosphorus oxide (< 20%), 2-Propenoic acid, 2-methyl-, 3-(triethoxysilyl)propyl ester, reaction products with silica and 3 (triethoxysilyl)-1-propanamine (5–15%), Ethanol (5–15%), water (5–15%), synthetic amorphous silica fumed, crystalline-free (< 10%), Methacrylic Acid, 3-(Triethoxysilyl) Propyl Ester (< 5%), Camphorquinone (< 2%), Copolymer of Acrylic and Itaconic Acid (< 2%), N, N-Dimethylbenzocaine (< 2%), (3-aminopropyl)triethoxysilane (< 0.5%), Diethylene glycol mimethacrylaye (< 0.5%), Acetic acid, copper (2+) salt, monohydrate (< 0.1%)
Flowable Resin composite	Filtek Supreme Flowable Restorative A3 (9571262)	3 M, ESPE, St. Paul, MN, USA	Bisphenol A Diglycidyl Ether Dimethacrylate (BISGMA) (5–10%), Triethylene Glycol Dimethacrylate (TEGDMA) (< 10%), BisPMA, Silane treated ceramic filler (50–60%), Silane Treated Silica (5–10%) Ytterbium Fluoride (YbF3) (1–5%), Diphenyliodonium Hexafluorophosphate (0.2%), Poly[oxy(1-oxo-1,6-hexanediyl)], α,α′-(oxydi-2,1-ethanediyl)bis[ω-[[[[2-[(2-methyl-1-oxo-2-propen-1-yl)oxy]ethyl]amino]carbonyl]oxy]- (1–5%), N, N-demethylbenzocaine (< 0.3%), Diphenyliodonium Hexafluorophosphate (< 0.2%)
Solvent	Isopropyl alcohol (1.00983.2500)	Merck KGaA, Darmstadt, Germany	Isopropanol or 2-propanol 99.5%
	Methyl ether ketone (2106844)	Fisher Scientific UK Ltd. Loughborough, UK	Methyl ether ketone 99.8%
	Tetrehydrofuran (00307)	Loba Chemie PVT Ltd.,Mumbai, India	Tetrahydrofuran 99.8%
Airborne-particle abrasion materials	Cobra (15911305)	Renfert GmbH, hilzingen, Germany	50-µm aluminum oxide particle 99.5%

Abbreviations: EDMA, polymerized ethylene dimethacrylate; BisGMA, bisphenol A-glycidyl methacrylate; TEGDMA, triethylene glycol dimethacrylate; UDMA, urethane dimethacrylate; BisEMA, bisphenol A ethoxylated dimethacrylate; BisPMA, 2,2-Bis-(4-(3 methacryloxypropoxy) phenyl) propane

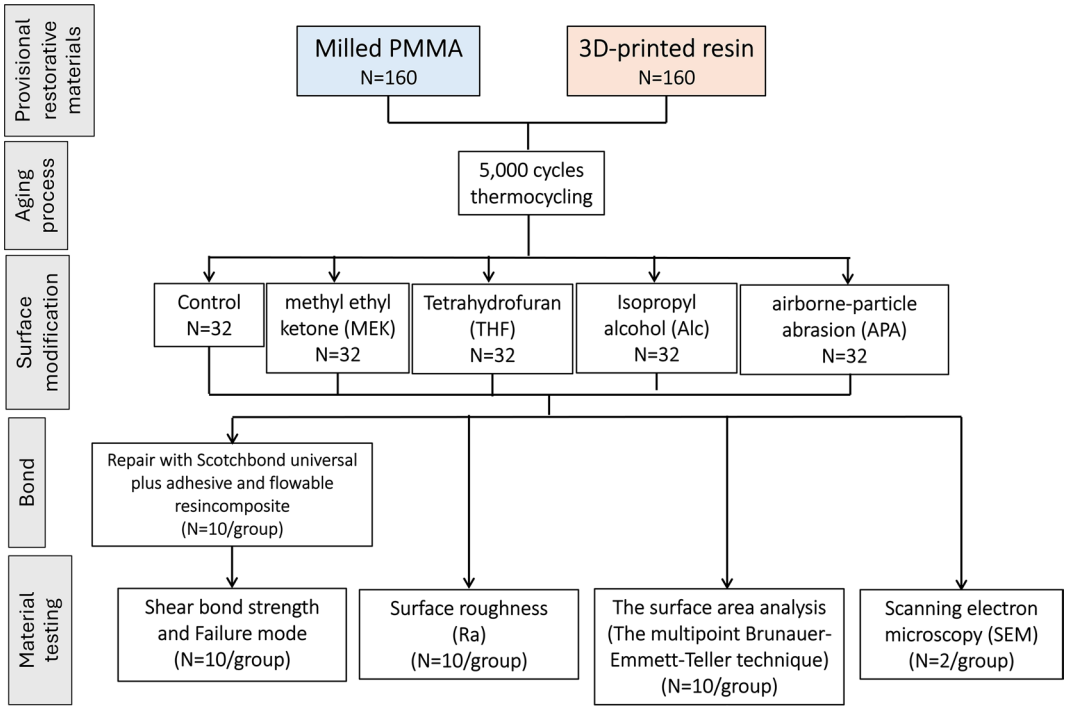

Fig. 1 Schematic samples and experimental flow chart

were polished with 600-, 800-, and 1,000-grit silicon carbide abrasive sheets. The dimensions of the samples were measured with a digital Vernier caliper (Digital ABS AOS Caliper; Mitutoyo Corp., Tokyo, Japan), and the samples were subsequently cleaned with deionized water in an ultrasonic bath for 10 min and air-dried. The provisional restorative materials received thermocycling for 5,000 cycles (SD Mechatronic, Feldkirchen-Westerham, Germany) between 5 °C and 55 °C, with a dwell time of 60 s in each water immersion [20]. All the samples were stored in a dry location after the aging procedure was complete.

Surface modifications

Each CAD/CAM material was embedded in a polyvinylchloride tube using an epoxy resin and randomly allocated into five groups ($N = 10$ per group) according to surface modification protocols:

Control: No surface modification.

MEK: The specimen surfaces were gently applied with a single layer of methyl ethyl ketone by a disposable microbrush for 60 s, rinsed with deionized water, and desiccated using oil-free air.

THF: The specimen surfaces were gently applied with a single layer of tetrahydrofuran by a disposable microbrush for 60 s, rinsed with deionized water, and desiccated using oil-free air.

IPA: The specimen surfaces were gently applied with a single layer of isopropyl alcohol by a disposable microbrush for 60 s, rinsed with deionized water, and desiccated using oil-free air.

APA: The specimen surfaces were treated with airborne-particle abrasion at a pressure of 1.5 bar for 10 s in a 10 mm perpendicular direction, utilizing 50 µm aluminum oxide (Cobra, hilzingen, Germany, Germany). Following a rinsing with deionized water, the surface was desiccated using oil-free air.

Following surface modification, all specimens were placed in a dry place prior to the subsequent operation.

Shear bond strength test and failure mode

Shear bond strength was tested according to the International Organization for Standardization (ISO 10477:2020) Dentistry - Polymer-based crown and veneering materials [21]. Following surface modification, a resin adhesive (Scotchbond universal plus adhesive; 3 M ESPE, St. Paul, MN, USA) was applied onto the sample surface using a microbrush. Then, they were air-dried for 20 s and light-cured (Elipar™ S 10. 3 M ESPE, St. Pual, MN, USA) for 20 s. Adhesive tape with a 2-mm-diameter bonding area was attached to the sample surface. All the samples were mounted into an Ultradent shear bond kit (Ultradent Products, South Jordan, UT, USA), which was composed of a bonding clamp and a mold inserted as shown in Fig. 2. A flowable resin composite (Filtek Z350 XT, 3 M ESPS, St. Paul, MN, USA) was then injected into a mold 2.38 mm in diameter and 2 mm in height, which was placed on top of the sample surface, followed by 40 s of

Fig. 2 Ultradent shear bond kit and samples used in this study

light curing. The samples were stored in distilled water at 37 °C for 1 day prior to shear bond strength testing.

Shear bond strength was assessed using a universal testing machine (EZ-S 500 N, Shimadzu Corporation, Kyoto, Japan) with a notched-edged shape shearing blade with a 1 mm/min crosshead speed. The shear bond strength value was calculated in MPa.

The debonded surface was observed under a ×40 magnification stereomicroscope (Olympus SZX16, Olympus, Tokyo, Japan.) Image analysis software (ImageJ 1.41, Wayne Rasband, National Institutes of Health, Bethesda, MD, USA) was used to determine the surface area. The type of failure was categorized as mixed, adhesive, or cohesive, as in previous studies [17, 19]. Cohesive failure was indicated when the composite resin or CAD/CAM provisional material substrate was observed in more than 60% of the total bonding area. If cohesive failure area was 40–60% of the total area, the materials were classified as having a mixed failure rate. The samples were characterized as experiencing adhesive failure if these areas comprised less than 40% of the total area.

Evaluating the modified surface of provisional restorative materials

The evaluation of the surface properties of provisional restorative materials after surface modification involves surface roughness, morphology, and specific surface area analysis.

Surface roughness and morphology analysis

To determine surface roughness (Ra), a noncontact surface roughness analyzer (Infinite Focus SL, Alicona Imaging GmbH, Graz, Austria) was used. The center of each modification group sample ($N = 10$ per group) was determined at 50x magnification. The data were analyzed via MetMaX software (version 4.0, Alicona, Austria). The surface roughness measurements of the traced areas were used in the following statistical analysis. The surface roughness values of the traced areas were employed in the subsequent statistical analyses.

The specific surface area analysis (the multipoint Brunauer-Emmett-Teller technique)

A high-performance adsorption analyzer using the multipoint Brunauer–Emmett–Teller technique or BET (3Flex, Micromeritics) was used to determine the specific surface area of each surface modification group ($N = 10$ per group). The samples were analyzed via nitrogen adsorption–desorption isotherms. Before the adsorption measurements were conducted, all materials were outgassed in the degas inlet of the adsorption analyzer for 48 h at 40 °C. The mathematical calculations described by the BET (Brunauer–Emmett–Teller) theory were used to analyze the specified surface area.

Scanning electron microscope (SEM) evaluation

For morphological analysis of the surface, two samples of each type of post that underwent surface treatments were analyzed using SEM. This was accomplished by employing a gold coater (Gold sputtering unit, JEOL Ltd., Akishima, Japan) and observing the samples at a magnification of 1000× using a scanning electron microscope (FEI Quanta 200, FEI Company, Netherland).

Data analysis

The data were analyzed using a statistical software program (SPSS for Windows version 22.0; SPSS Inc., Chicago, IL, USA) at the 5% significance level. Data normality and equal variance were confirmed by the Shapiro–Wilk and Levene tests. The effects of material type and surface modification protocol on the SBS, surface roughness and specific surface area were analyzed via two-way analysis of variance (ANOVA), followed by the Bonferroni post hoc correction.

Results

Two-way ANOVA revealed an interaction effect between 3D-printed resin and milled PMMA restorative materials and surface modification protocols on SBS, surface roughness and specific surface area.

Shear bond strength

SBS results are shown in Fig. 3 and indicate that for the 3D-printed resin, the mean (95% confidence interval) SBS values (MPa) of MEK [23.2 (21.1–25.2), THF [27.2 (26.0–28.5)], and APA [27.9 (26.1–29.8)] groups were significantly greater than did the Alc [16.1 (14.4–17.7)] and control [11.7 (10.3–12.9)] groups. Similarly, for milled PMMA, the SBS values were significantly greater

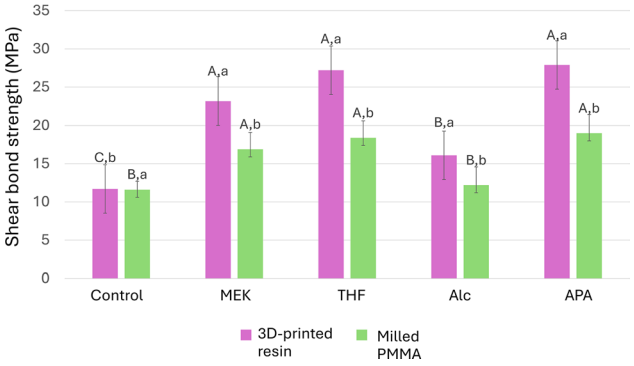

Fig. 3 Mean and standard deviation (SD) of shear bond strength (SBS) for each surface modification group in aged 3D-printed resin and milled PMMA. Identical uppercase letters within the same material type (either 3D-printed resin or milled PMMA) indicate no statistically significant differences ($p > 0.05$) between different surface modifications. Non-identical uppercase letters indicate statistically significant differences ($p < 0.05$) among surface modifications within the same material. Similarly, non-identical lowercase letters within each surface modification group indicate statistically significant differences ($p < 0.05$) between 3D-printed resin and milled PMMA

in the MEK [16.9 (15.3–18.5)], THF [18.4 (16.8–20.0)], and APA [19.0 (17.2–20.7)] groups than in the Alc [12.2 (10.5–13.9)] and control [11.6 (10.8–12.4)] groups. In a comparison of the 3D-printed resin and milled PMMA, all surface modification groups in the 3D-printed resin demonstrated significantly higher SBSs than their counterparts in milled PMMA. However, in the control group, milled PMMA resulted in significantly higher SBS than did the 3D-printed resin.

Failure mode

The results of the failure analysis are depicted in Fig. 4, and an example of the sample is shown in Fig. 5. The failure mode analysis revealed no differences between milled PMMA and 3D-printed resin materials under the same surface modification in the control and Alc groups; both milled PMMA and 3D-printed resin exhibited total adhesive failure. The APA group exhibited 50% cohesive failure, and the THF and MEK groups demonstrated 20% cohesive failure in both the 3D-printed resin and milled PMMA. Conversely, the THF and MEK groups of 3D-printed resin presented a 30% mixed failure rate, whereas the milled PMMA group, with the THF and MEK groups, presented a 10% mixed failure rate.

SEM analysis

The SEM results shown in Fig. 6 indicate that all surface modifications can alter the surface topography; the THF and MEK groups presented distinctive rougher surface morphologies than did the Alc group of both provisional restorative materials. The milled PMMA has a void on the surface, as represented by the red arrows. The 3D-printed resin had homogenous surface morphology. Considering the surface modification, in the milled PMMA group, the solvent modification groups had a larger void size than did the control group.

Surface roughness results

The surface roughness results are shown in Table 2. Representative images of the samples captured via a 3D digital microscope are shown on Fig. 7.

Within the 3D-printed resin, the mean (95% CI) surface roughness value (μm) of APA group was the highest [1834.2 (1803.8–1864 μm)], followed by the THF [393.8 (386.3–401.3)] and MEK groups [383.5 (375.7–389.4)], which demonstrated no statistically significant difference between them, followed by the Alc [258.4 (253.7–263.0)] and control groups [252.1 (248.6–255.5)], which have the lowest value. Among the milled PMMA samples, the APA group [1052.8 (1027.0–1078.5)] also presented the highest surface roughness values, followed by the MEK [498.1

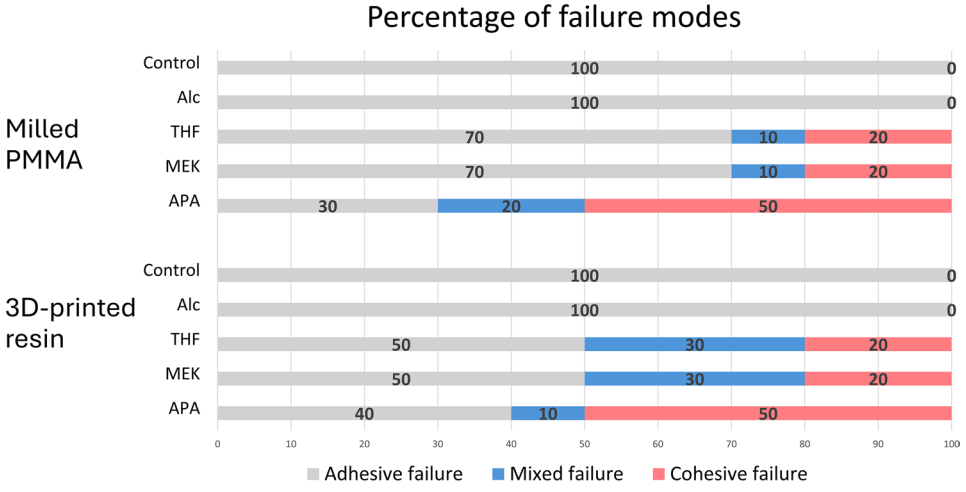

Fig. 4 Bar chart showing the distribution of failure modes in this study

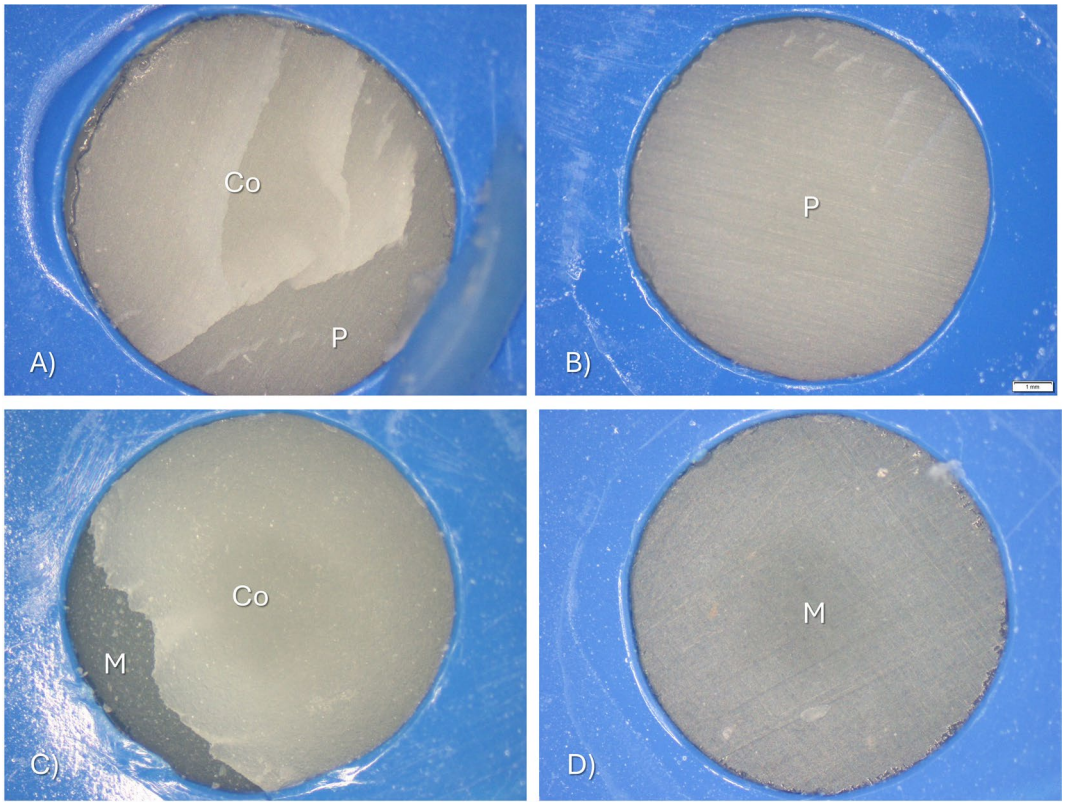

Fig. 5 Examples of the samples from different groups, which were used to analyze the failure patterns with a scanning electron microscope. (**A**) and (**B**) 3D-printed resin samples repaired with a flowable resin composite. (**A**) Cohesive failure and (**B**) adhesive failure. (**C**) and (**D**) Milled PMMA repaired with a flowable resin composite. (**C**) An adhesive failure and (**D**) an adhesive failure. Note: Co: resin composite, P: 3D-printed resin, M: milled PMMA

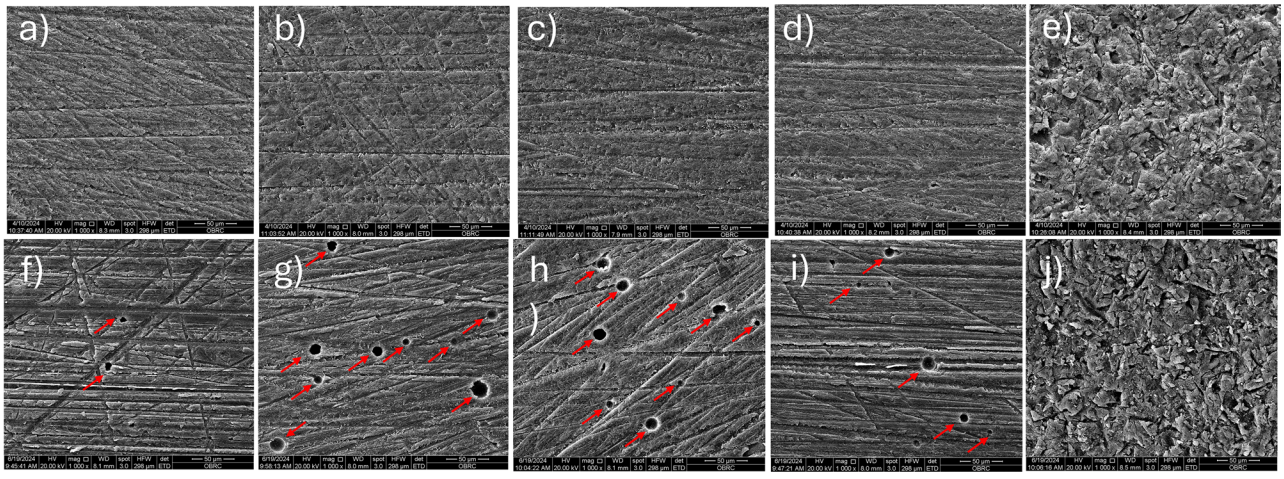

Fig. 6 SEM images (×500) showing the surface topography of the 3D-printed resin (**a**-**e**) and milled PMMA (**f**-**j**); the control (**a** and **f**) and surface modification groups included methyl ether ketone (**b** and **g**), tetrahydrofuran (**c** and **h**), and isopropyl alcohol (**d** and **i**) after 60 min of application and airborne-particle abrasion (**e** and **j**). Note the pores in the milled PMMA (red arrows)

(488.5–507.7)] and THF groups [490.1 (482.1–498.3)], which demonstrated no statistically significant difference. The control group [349.3 (341.8–356.8)] and the Alc group [348.6 (342.0–355.1)] had the lowest values. Compared to 3D-printed resin, milled PMMA appears to have a higher surface roughness within the same surface modification group, except for the APA group.

Specific surface area analysis

Considering the specific surface area value, the result is different than the surface roughness, as shown in Table 2.

Table 2 Mean (SD) surface roughness and specific surface area (BET) of 3D-printed resin and milled PMMA

		Control	MEK	THF	Alc	APA
Surface roughness (μm)	3D-Printed resin	252.1 (4.82)$^{C, b}$	383.5 (9.59)$^{B, b}$	393.8 (10.5)$^{B, b}$	258.4 (6.54)$^{C, b}$	1834.2 (42.5)$^{A, a}$
	Milled PMMA	349.3 (10.5)$^{C, a}$	498.1 (13.5)$^{B, a}$	490.1 (11.3)$^{B, a}$	348.6 (9.18)$^{C, a}$	1052.8 (36.0)$^{A, b}$
Specific surface area (m^2/g)	3D-Printed resin	2.18 (0.06)$^{C, b}$	4.83 (0.08)$^{A, b}$	4.95 (0.16)$^{A, b}$	2.21 (0.14)$^{C, b}$	4.45 (0.24)$^{B, b}$
	Milled PMMA	3.15 (0.04)$^{B, a}$	5.18 (0.10)$^{A, a}$	5.22 (0.06)$^{A, a}$	3.15 (0.07)$^{B, a}$	5.17 (0.13)$^{A, a}$

Identical uppercase letters in each row (horizontally) indicate no statistically significant differences ($p > 0.05$), whereas nonidentical letters in each row indicate statistically significant differences ($p < 0.05$). The identical lowercase letters in each column (vertically) indicate statistically significant differences ($p < 0.05$) between the 3D-printed resin and milled PMMA

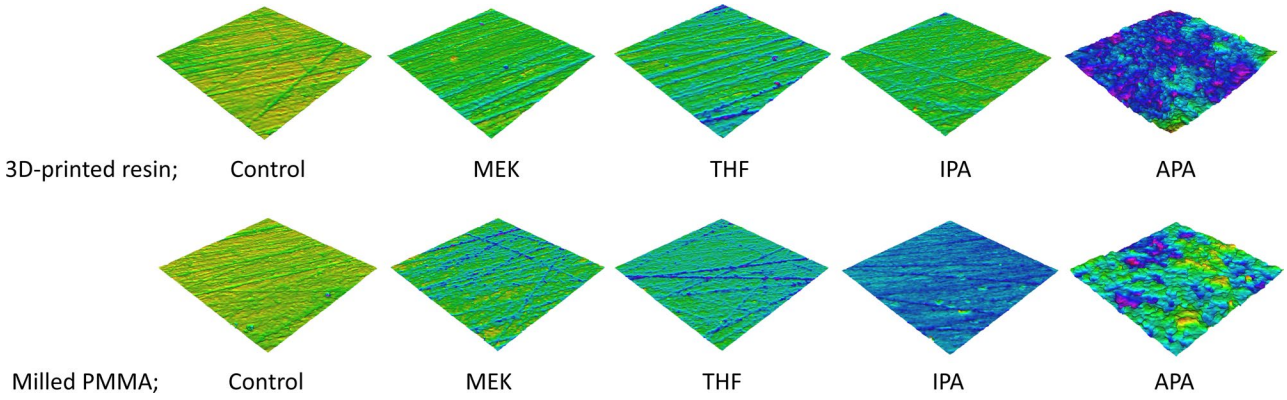

Fig. 7 The surface topography of 3D-printed resin and milled PMMA after surface modification

Among the 3D-printed resins, the mean (95% CI) of specific surface area (m^2/g) of THF group was the highest [4.95 (4.84–5.07)] presented the highest, with no statistically significant difference in the MEK group [4.83 (4.77–4.89)], followed by the APA [4.45 (4.29–4.62), Alc [2.21 (2.11–2.30), and control groups [2.18 (2.13–2.22)]. Among the milled PMMA samples, the THF group [5.22 (5.18–5.26)] had the highest specific surface area; however, the specific surface area was not significantly different from that of the MEK [5.18 (5.11–5.25)] and APA groups [5.17 (5.07–5.26)], followed by the Alc [3.15 (3.13–3.18)] and control groups [3.15 (3.10–3.20)]. In the same surface modification groups, milled PMMA results in greater surface roughness than 3D-printed resin.

Discussion

The repairability of CAD/CAM provisional restorative materials is essential, as it determines the successful outcome of fixed prosthodontic treatment. This study demonstrated the reparability of the differences in shear bond strength resulting from different surface modification techniques. Therefore, the null hypothesis is rejected.

In laboratory investigations, thermocycling has been employed to imitate the aging process of composite resins. Contrasting to other aging procedures, such as storage in water immersion. Thermocycling is a method that combines the processes of thermal and hydrolysis degradations by subjecting materials to repeated immediate temperature swings to stimulate the breakdown caused by temperature changes [20].

This research used thermocycling for 5,000 cycles for the aging method since this duration corresponds to a usage duration of six months [20, 22, 23]. The 5,000 cycles are the same as in previous studies [24], which is considered the maximum used period for provisional restorations. Additionally, it directly weakens the interface between the matrix and filler by undergoing hydrolytic degradation of the silane/filler interface and the surface of the filler particles [25]. Research has indicated that 3D-printed resins demonstrate substantially greater shear bond strength (SBS) than milled PMMA does, possibly contributing to their greater susceptibility to solvent dissolution. Susceptibility is affected by the similarity in solubility parameters between the resin and solvents [26, 27].

Solvents are substances capable of dissolving and dispersing one or more solutes, enabling the formation of a solution. During the dissolution of a solid or liquid, solvents work by separating the space between solute molecules or ions. A key scientific parameter in this process is cohesive energy, which represents the energy required to break the bonds between solute molecules [26, 27]. If the solubility parameters of the solvent and the solute are similar, the solvent can penetrate the polymer structure, leading to swelling and softening of the resin matrix, hence facilitating monomer impregnation from bonding agents into the polymer network [27, 28]. Although

3D-printed resins, consisting of methacrylate monomers, oligomers, and fillers, lack comprehensive solubility parameter data, PMMA, the primary constituent of milled materials, has a solubility parameter of 18.7 MPa½ [29]. Solvents such as isopropyl alcohol, tetrahydrofuran, and methyl ethyl ketone, with values of 26, 18.6, and 19.4 MPa½ respectively [29, 30], affect the dissolution and bonding performance of these materials. Considering the failure analysis, in the 3D-printed resin, the THF and MEK groups presented a higher percentage of mixed failure than did the milled PMMA group, confirming that the 3D-printed resin is susceptible to solvent. The higher rate of mixed and cohesive failure suggests that the bonding interphase is highly successful until fracture occurs within the material.

SEM revealed significant differences in surface morphology between PMMA milled materials and 3D-printed resin materials. The surface modification of the 3D-printed resin was prominent and apparent because of interactions between the solvent and the polymer surface. In the milled PMMA group, pores generally appeared in all the samples. In contrast, a previous study reported that milled PMMA has fewer voids and spaces, which results in a lower roughness than 3D-printed resin [31]. However, this finding implies that the varying densities of fabricating materials used by manufacturers may have contributed to the porosity of milled PMMA [32], which in turn produced porosities among different CAD/CAM PMMA brands. After the solvent modification, a pore became more apparent and expanded on the surface, as illustrated by the red arrow in Fig. 7.

With respect to surface roughness, the APA group had the highest roughness. However, this does not correspond with the shear bond strength value, as the chemical surface modification using MEK and THF similarly provides the highest shear bond strength, similar to that of APA. To demonstrate the impact of solvent on swelling and spacing for monomer penetration, we conducted a specific surface area analysis. This analysis utilized the BET method, which utilizes adsorption isotherms of nonreactive nitrogen to determine the interstitial surface area of the pores per unit of bulk volume [33]. In dental research, the BET method was introduced for evaluating the porosity of etched human enamel [34, 35].

The analysis of the specific surface area indicated that THF and APA resulted in the highest specific surface areas. This study revealed that polymer matrix swelling, and dissolution alters surface morphology. Compared with APA, solvent modifications can impact outcomes. A recent study demonstrated that APA is successful in removing surface contaminants, which is important because creating a fresh and clean surface is essential for desirable bonding [36].

However, solvent surface modification using THF and MEK can improve the strength of the repair bond just as significantly as the APA technique. A previous study revealed that APA had a damaging effect on CAD/CAM composite materials, leading to the formation of subsurface cracks of restorative materials [37]. Contrasting solvent application, which is characterized by quick evaporation and enables fine control over areas that can avoid the compromised regions of repair. This study highlights the therapeutic significance of solvent surface modification, particularly the use of THF and MEK in comparison to APA.

In general, the solvent has an important role in primer/adhesive processes by allowing the dissolution and diffusion of monomers in dentine substrates. The solvents that are usually incorporated in dental adhesives include water, ethanol and acetone. Conversely, few studies have investigated the application of solvents such as THF and MEK to modify composite surfaces [17, 18].

This study is limited as it focused solely on the immediate shear bond strength of aged CAD/CAM provisional restorative materials. Future research must include thermocycling on repaired specimens to accurately assess the efficacy of bond strength throughout usage durations. The aging approach in this study was limited to the thermocycling approach, excluding alternative methods such as mechanical loading or immersion solutions. Additionally, previously mentioned topics must be taken into consideration in the next experimental framework as they are essential to the development of therapeutic treatment regimens.

Conclusion

In conclusion, surface modification with THF, MEK and APA improved repairability, hence increasing the shear bonding strength of the flowable composite to milled PMMA and 3D-printed resin provisional restorative materials compared with that of the Alc application and control group. SEM analysis, surface roughness, and specific surface area analyses revealed alterations in the surface morphology of both provisional restorative materials caused by solvent exposure, which corresponds with the shear bond strength results.

Abbreviations

Alc	Isopropyl Alcohol Application
APA	Airborne-Particle Abrasion
BET	Brunauer–Emmett–Teller
BisGMA	Bisphenol A-Glycidyl Methacrylate
BisEMA	Bisphenol A Ethoxylated Dimethacrylate
BisPMA	2,2-Bis-(4-(3 methacryloxypropoxy) phenyl) propane
CAD/CAM	Computer-Aided Design and Computer-Aided Manufacturing
EDMA	Polymerized Ethylene Dimethacrylate
MEK	Methyl Ethyl Ketone
THF	Tetrahydrofuran
PMMA	Polymethylmethacrylate

Acknowledgements
This study was supported by the Office of Research Affairs, Faculty of Dentistry, Chulalongkorn University.

Author contributions
P.C., W.P.: established the fundamental research design and contributed to the writing of the manuscript; P.C., N.L.: established the fundamental research framework, conducted data analysis, and assessed quality; P.C.,W.P.: conducted sample preparation and characterization; P.C.,W.P., N.L., A.K., P.U., K.B.: manuscript formatting and revision; All the authors reviewed and endorsed the text and confirmed its accuracy.

Funding
Not applicable.

Data availability
The data supporting the results of this investigation are available from the corresponding author upon reasonable request.

Declarations

Ethics approval and consent to participate
Not applicable.

Consent for publication
Not applicable.

Competing interests
The authors declare no competing interests.

Author details
[1]Vejthani Hospital, Bangkok 10240, Thailand
[2]Department of Prosthodontics, Faculty of Dentistry, Chulalongkorn University, 34 Henri-Dunant Road, Wangmai, Pathumwan, Bangkok 10330, Thailand
[3]Department of Restorative Dentistry, Faculty of Dentistry, Naresuan University, Phitsanulok, Thailand
[4]Department of Prosthodontics, Faculty of Dentistry, Khon Kaen University, Khon Kaen 40002, Thailand
[5]Division of Prosthodontics, Faculty of Dentistry, Thammasat University, Pathumthani 12120, Thailand

Received: 19 December 2024 / Accepted: 27 February 2025
Published online: 11 March 2025

References

1. Field J, Wassell R. Provisional restorations (Part 1). Br Dent J. 2023;234(11):805–9.
2. Strub JR, Rekow ED, Witkowski S. Computer-aided design and fabrication of dental restorations: current systems and future possibilities. J Am Dent Assoc. 2006;137(9):1289–96.
3. Jeong KW, Kim SH. Influence of surface treatments and repair materials on the shear bond strength of CAD/CAM provisional restorations. J Adv Prosthodont. 2019;11(2):95–104.
4. Ruse ND, Sadoun MJ. Resin-composite blocks for dental CAD/CAM applications. J Dent Res. 2014;93(12):1232–4.
5. Della Bona A, Cantelli V, Britto VT, Collares KF, Stansbury JW. 3D printing restorative materials using a stereolithographic technique: a systematic review. Dent Mater. 2021;37(2):336–50.
6. Lodding DW. Long-term esthetic provisional restorations in dentistry. Curr Opin Cosmet Dent. 1997;4:16–21.
7. Rayyan MM, Aboushelib M, Sayed NM, Ibrahim A, Jimbo R. Comparison of interim restorations fabricated by CAD/CAM with those fabricated manually. J Prosthet Dent. 2015;114:414–9.
8. Bohnenkamp DM, Garcia LT. Repair of bis-acryl provisional restorations using flowable composite resin. J Prosthet Dent. 2004;92(5):500–2.
9. Lim NK, Shin SY. Bonding of conventional provisional resin to 3D printed resin: the role of surface treatments and type of repair resins. J Adv Prosthodont. 2020;12(5):322–8.
10. Palavicini J, Quin SL, Zakkour W, et al. Bond strength of Reline materials to 3D-Printed provisional crown resins. Polymers. 2023;15(18):3745.
11. Wiegand A, Stucki L, Hoffmann R, Attin T, Stawarczyk B. Repairability of CAD/CAM high-density PMMA- and composite-based polymers. Clin Oral Investig. 2015;19(8):2007–13.
12. Sismanoglu S, Yildirim-Bilmez Z, Erten-Taysi A, Ercal P. Influence of different surface treatments and universal adhesives on the repair of CAD-CAM composite resins: an in vitro study. J Prosthet Dent. 2020;124(2):e2381–9.
13. Dewan H, Sayed ME, Jundus A, Gharawi M, Baeshen S, Alali M, et al. Shear strength of repaired 3D-printed and milled provisional materials using different resin materials with and without chemical and mechanical surface treatment. Polymers. 2023;15(21):4284.
14. Irmak Ö, Baltacıoğlu İH, Ulusoy N, Bağış YH. Solvent type influences bond strength to air or blot-dried dentin. BMC Oral Health. 2016;16(1):77.
15. Ekambaram M, Yiu CKY, Matinlinna JP. An overview of solvents in resin-dentin bonding. Int J Adhes Adhes. 2015;57:22–33.
16. Fontes ST, Fernández MR, Ogliari FA, et al. Tetrahydrofuran as solvent in dental adhesives: cytotoxicity and dentin bond stability. Clin Oral Investig. 2013;17(1):237–42. https://doi.org/10.1007/s00784-012-0693-5.
17. Prawatvatchara W, Angkanawiriyarak S, Klaisiri A, Sriamporn T, Thamrongananskul N. Effect of Aprotic solvents on the microtensile bond strength of composite core and fiber-reinforced composite posts. Polymers. 2023;15(19):3984.
18. Bunchansakul N, Thamrongananskul N. The effect of surface treatment on shear bond strength of resin matrix ceramics and dual cure resin cement. J Int Dent Med Res. 2020;13:1248–57.
19. Klaisiri A, Suebnukarn S, Krajangta N, Rakmanee T, Sriamporn T, Thamrongananskul N. The effect of morpholine on composite-to-composite repair strength contaminated with saliva. Polymers. 2022;14(21):4718.
20. Gale MS, Darvell BW. Thermal cycling procedures for laboratory testing of dental restorations. J Dent. 1999;66:1336–9.
21. ISO 10477:2020. Dentistry-Polymer-based crown and veneering materials. Switzerland. 2020.
22. Rinastiti M, Özcan M, Siswomihardjo W, Busscher HJ. Effects of surface conditioning on repair bond strengths of non-aged and aged microhybrid, nanohybrid, and nanofilled composite resins. Clin Oral Investig. 2011;15(5):625–33.
23. Özcan M, Barbosa S, Melo R, Galhano G, Bottino M. Effect of surface conditioning methods on the microtensile bond strength of resin composite to composite after aging conditions. Dent Mater. 2007;23:1276–82.
24. Reeponmaha T, Angwaravong O, Angwarawong T. Comparison of fracture strength after thermo-mechanical aging between provisional crowns made with CAD/CAM and conventional method. J Adv Prosthodont. 2020;12(4):218–24. https://doi.org/10.4047/jap.2020.12.4.218.
25. Ellakany P, Fouda SM, Mahrous AA, AlGhamdi MA, Aly NM. Influence of CAD/CAM milling and 3D-Printing fabrication methods on the mechanical properties of 3-Unit interim fixed dental prosthesis after Thermo-Mechanical aging process. Polymers. 2022;14(19):4103.
26. Mabesoone MFJ, Palmans ARA, Meijer EW. Solute-Solvent interactions in modern physical organic chemistry: supramolecular polymers as a muse. J Am Chem Soc. 2020;142(47):19781–98.
27. Miller-Chou BA, Koenig JL. A review of polymer dissolution. Prog Polym Sci. 2003;28:1223–70.
28. Vallittu PK, Ruyter IE, Nat R. The swelling phenomenon of acrylic resin polymer teeth at the interface with denture base polymers. J Prosthet Dent. 1997;78(2):194–9.
29. Marianne G, editor. Brydson's plastics materials: relation of structure to chemical properties. 8 ed. th ed. Oxford: Butterworth-Heinemann; 2017. pp. 75–105.
30. Hansen CM. Hansen solubility parameters. A user's handbook. 2nd ed. Boca Raton: CRC; 2007. pp. 1–43.
31. Abdul-Monem MM, Hanno KI. Effect of thermocycling on surface topography and fracture toughness of milled and additively manufactured denture base materials: an in-vitro study. BMC Oral Health. 2024;24(1):267.
32. Steinmassl PA, Wiedemair V, Huck C, Klaunzer F, Steinmassl O, Grunert I, Dumfahrt H. Do CAD/CAM dentures really release less monomer than conventional dentures? Clin Oral Investig. 2017;21(5):1697–705.
33. Naderi M. Chapter Fourteen-Surface area: Brunauer-Emmett-Teller (BET). In: Tarleton ES, editor. Progress in filtration and separation. Cambridge: Academic; 2015. pp. 585–608.
34. Orellana MF, Nelson AE, Carey JP, Heo G, Boychuk DG, Major PW. Surface analysis of etched molar enamel by gas adsorption. J Dent Res. 2008;87(6):532–6.

35. Nguyen TT, Miller A, Orellana MF. Characterization of the porosity of human dental enamel and shear bond strength in vitro after variable etch times: initial findings using the BET method. Angle Orthod. 2011;81(4):707–15.
36. Yang B, Wolfart S, Scharnberg M, Ludwig K, Adelung R, Kern M. Influence of contamination on zirconia ceramic bonding. J Dent Res. 2007;86(8):749–53.
37. Yoshihara K, Nagaoka N, Maruo Y, et al. Sandblasting May damage the surface of composite CAD-CAM blocks. Dent Mater. 2017;33(3):e124–35.

Publisher's note